



# Aminoalkyl-substituted flavonoids: synthesis, cholinesterase inhibition, $\beta$ -amyloid aggregation, and neuroprotective study

Laleh Faraji<sup>1</sup> · Hamid Nadri<sup>2</sup> · Alireza Moradi<sup>2</sup> · Syed Nasir Abbas Bukhari<sup>3</sup> · Bahar Pakseresht<sup>4</sup> · Farshad Homayouni Moghadam<sup>5</sup> · Setareh Moghimi<sup>1</sup> · Mohammad Abdollahi<sup>1,6</sup> · Mehdi Khoobi<sup>1,7</sup> · Alireza Foroumadi<sup>8,9</sup>

Received: 26 December 2018 / Accepted: 22 April 2019 / Published online: 23 May 2019  
© Springer Science+Business Media, LLC, part of Springer Nature 2019

## Abstract

In this manuscript, 17 aminoalkyl-substituted flavonoid derivatives were synthesized and their anticholinesterase, anti-beta-amyloid (A $\beta$ ) aggregation and neuroprotective activities were evaluated. The synthesized compounds were prepared through four-step reaction, started from the reaction between 2-hydroxyacetophenone and 4-methoxy benzaldehyde. Among the final compounds, **6j** displayed the best anti-butyrylcholinesterase activity (IC<sub>50</sub> = 0.335  $\mu$ M). Moreover, compound **6i** significantly protected PC12 neurons against H<sub>2</sub>O<sub>2</sub>-induced cell death. This compound could also inhibit acetylcholinesterase and self-induced A $\beta$  peptide aggregation by 51.3% and 49.2%, respectively. The results indicated that compound **6i** could be considered as a lead compound towards the discovery of disease-modifying drugs for Alzheimer's disease (AD) therapy.

**Keywords** Alzheimer's disease · Flavonoid · Synthetic chemistry

## Introduction

Alzheimer's disease (AD), the most common cause of mental deterioration in people with advanced ages, is a neurodegenerative disorder, characterized by severe behavioral abnormalities, decline in memory and cognitive capabilities (Piazzini et al. 2003; Scarpini et al. 2003). Despite the unclear character of AD's etiology, a variety of factors

such as low levels of acetylcholine (ACh), oxidative stress, formation of amyloid  $\beta$ -protein (A $\beta$ ) plaques, and abnormal posttranslational modifications of tau protein are considered in the pathophysiology of the disease (Masters et al. 1985; Tumiatti et al. 2010; Yankner et al. 1989). Relying on this fact, multi-target directed ligands (MTDLs) treatment strategy has emerged as a promising approach to develop novel anti-Alzheimer agents.

Acetylcholinesterase (AChE) and butyrylcholinesterase (BuChE) are two responsible species in hydrolysis of the ACh, the first identified cholinergic neurotransmitter. Clinically approved drugs, tacrine, donepezil, galantamine,

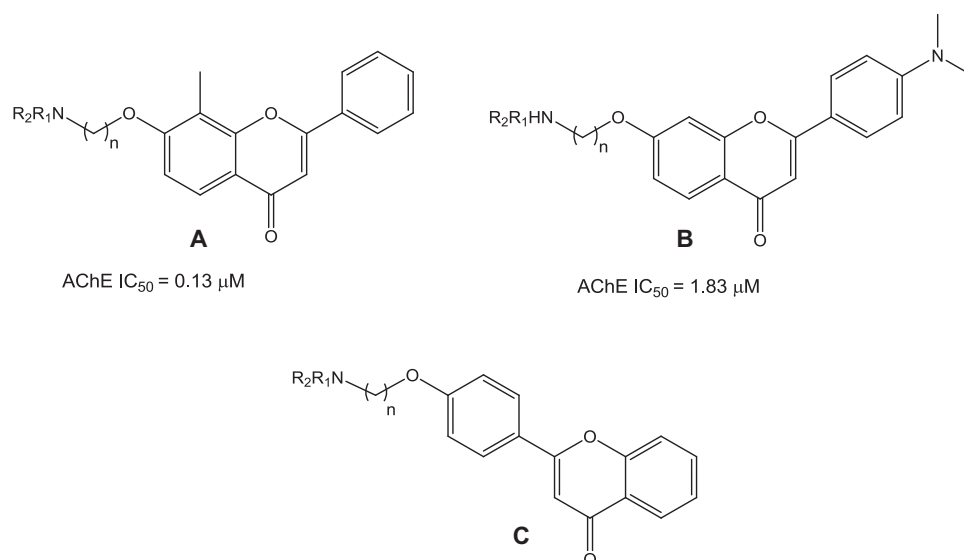
**Supplementary information** The online version of this article (<https://doi.org/10.1007/s00044-019-02350-4>) contains supplementary material, which is available to authorized users.

- ✉ Mehdi Khoobi  
khoobi@tums.ac.ir
- ✉ Alireza Foroumadi  
aforoumadi@yahoo.com

- <sup>1</sup> The Institute of Pharmaceutical Sciences (TIPS), Tehran University of Medical Sciences, Tehran, Iran
- <sup>2</sup> Department of Medicinal Chemistry, Faculty of Pharmacy, Shahid Sadoughi University of Medical Sciences, Yazd, Iran
- <sup>3</sup> Department of Pharmaceutical Chemistry, College of Pharmacy, Aljouf University, Aljouf, Sakaka 2014, Saudi Arabia
- <sup>4</sup> Department of Cellular Biotechnology, Cell Science Research

- Center, Royan Institute for Biotechnology, ACECR, Isfahan, Iran
- <sup>5</sup> Center of Excellence in Electrochemistry, Faculty of Chemistry, University of Tehran, Tehran, Iran
- <sup>6</sup> Department of Toxicology and Pharmacology, Faculty of Pharmacy, Tehran University of Medical Sciences, Tehran, Iran
- <sup>7</sup> Department of Pharmaceutical Biomaterials and Medical Biomaterials Research Center, Faculty of Pharmacy, Tehran University of Medical Sciences, Tehran, Iran
- <sup>8</sup> Neuroscience Research Center, Institute of Neuropharmacology, Kerman University of Medical Sciences, Kerman, Iran
- <sup>9</sup> Department of Medicinal Chemistry, Faculty of Pharmacy, Tehran University of Medical Sciences, Tehran, Iran

**Fig. 1** Structures of some known flavonoids derivatives (**a–c**) as cholinesterase inhibitors



and rivastigmine, offered an increased cholinergic transmission via inhibition of AChE (Bartus et al. 1982; Giacobini 2004; Xie et al. 2008) and induced an improvement in short-term memory and cognitive levels. The accumulative side effects and disadvantages of these drugs such as short half-life, periphery side effects, hepatotoxicity, and gastrointestinal tract disorders have encouraged researchers to develop more effective AChE inhibitors (Huang et al. 2010; Viau et al. 1993). The activity of AChE with the progression of AD reduced, while the levels of BuChE remained unchanged or increased with disease progression. Therefore, BuChE was also found effective in the regulation of ACh level. In this regard, the development of specific inhibitors capable of inhibiting both BuChE and AChE which can also interfere with aggregation of  $\beta$ -amyloid would be beneficial in clinical outcomes of AD (Greig et al. 2001; Luo et al. 2011).

Amyloid beta ( $A\beta$ ) is a soluble peptide, produced by cleavage of amyloid precursor protein, forming the amyloid plaques as markers of AD. Therefore,  $A\beta$  cascade could be considered as an important target in the treatment of AD (Hardy and Selkoe 2002; Inestrosa et al. 1996). In order to prevent disease progression, novel small molecules were synthesized based on known pharmacophores as cholinesterase inhibitors (Fernández-Busquets 2013; Panek et al. 2017; Selkoe 1999). Many studies showed that oxidative damage is an important factor in an initial progress of AD (Praticò 2008; Trippier et al. 2013). Therefore, the protection against oxidative stress by neuroprotective agents will be an appropriate treatment for AD (Longo and Massa 2004).

Flavonoids are a large family of polyphenolic compounds, naturally found in fruits and vegetables. The increased attention to the synthesis of this class of compounds is related to their numerous pharmacological

properties (He et al. 2012; Katalinic et al. 2010; Li et al. 2013a, 2013b; Sheng et al. 2009; Singh et al. 2014; Uriarte-Pueyo and Calvo 2011; Williams and Spencer 2012) such as antioxidant as well as AChE, BuChE, and  $A\beta$  fibril formation inhibitory activities (Lou et al. 2011). Some researchers have described the efficiency of flavonoid framework in the design of new AChE inhibitors. For instance, a series of flavonoid derivatives were synthesized as potential multifunctional ligands against AD with inhibitory potency against cholinesterases,  $A\beta$  self-aggregation, and metal-chelating ability. In another study, some amine substituted flavonoid derivatives (Fig. 1b, c) were synthesized as multitarget anti-AD agents with cholinesterase inhibitory, antioxidant, and self-induced  $A\beta$  aggregation inhibitory activities (Lu et al. 2016; Luo et al. 2013).

Regarding this platform, and in continuation of our previous works on the development of novel agents with multifunctional activities against AD (Alipour et al. 2014; Asadipour et al. 2013; Ghanei-Nasab et al. 2016; Jalili-Baleh et al. 2018; Mehrabi et al. 2017; Pourabdi et al. 2016), in this work we describe a new series of flavonoid-based compounds and evaluate their AChE and BuChE inhibitory activities,  $A\beta$  self- and AChE-induced aggregation, and their antioxidant potential for neuroprotection.

## Methods and materials

### General chemistry

Melting points were measured by a *Kofler* hot stage apparatus and are uncorrected. <sup>1</sup>H- and <sup>13</sup>C-NMR spectra were recorded on *Bruker FT-500* (Germany), using TMS as an internal standard. The IR spectra were obtained by a *Nicolet*

*Magna FTIR 550* spectrometer (KBr disks). The elemental analysis was performed with an Elementar Analyses system GmbH *VarioEL* CHNS mode (Germany). The progress of all reactions was monitored by TLC on precoated silica gel 60 F254 plates (Merck).

## General procedures

### General procedures for the preparation of intermediates (5a–c)

To a solution of intermediate **4** (1.19 g and 5.0 mmol) and anhydrous potassium carbonate (3.5 g and 25.0 mmol) in acetone (50 mL), dibromoalkane (20.0 mmol) was added. The mixture was refluxed under stirring for 6 h. After cooling, the mixture was filtered and the filtrate was evaporated under reduced pressure. The obtained residue was purified by column chromatography, eluting with hexane/ethyl acetate (20:1) to afford compound **5a–c**.

#### 2-(4-(3-Bromopropoxy)phenyl)-4H-chromen-4-one (5a)

Light pink solid; yield: 90%, m.p.: 123–125 °C; IR (KBr,  $\text{cm}^{-1}$ )  $\nu_{\text{max}}$ : 1634 (C=O);  $^1\text{H}$  NMR (DMSO- $d_6$ , 500 MHz)  $\delta$  (ppm): 8.07 (d,  $J = 8.7$  Hz, 2H,  $\text{H}_2'$ , and  $\text{H}_6'$ ), 8.04 (d,  $J = 8.2$  Hz, 1H,  $\text{H}_5$ ), 7.82 (t,  $J = 8.2$  Hz, 1H,  $\text{H}_7$ ), 7.76 (d,  $J = 8.2$  Hz, 1H,  $\text{H}_8$ ), 7.49 (t,  $J = 8.2$  Hz, 1H,  $\text{H}_6$ ), 7.15 (d,  $J = 8.7$  Hz, 2H,  $\text{H}_3$  and  $\text{H}_5'$ ), 6.94 (s, 1H,  $\text{H}_3$ ), 4.20 (t,  $J = 6.0$  Hz, 2H,  $\text{CH}_2\text{-O}$ ), 3.69 (t,  $J = 6.5$  Hz, 2H,  $\text{CH}_2\text{-Br}$ ), 2.32–2.27 (m, 2H,  $\text{CH}_2$  aliphatic chain);  $^{13}\text{C}$  NMR (DMSO- $d_6$ , 125 MHz)  $\delta$  (ppm): 176.8, 162.5, 161.2, 155.5, 134.0, 128.2, 125.3, 124.7, 123.4, 123.3, 118.3, 115.0, 105.4, 65.7, 31.7, 30.9; anal. calcd. for  $\text{C}_{18}\text{H}_{15}\text{BrO}_3$ : C, 60.18; H, 4.21; found: C, 60.43; H, 3.96.

### General procedures for the preparation of compounds (6a–q)

To a solution of corresponding intermediates **5a–c** (0.5 mmol) in dried acetonitrile (5 mL),  $\text{K}_2\text{CO}_3$  (2.5 mmol) and different amines (1.0 mmol) were added and the mixture was stirred at 80 °C for 10 h. After that, the mixture was filtered and the filtrate was concentrated under reduced pressure. The residue was dissolved in  $\text{CH}_3\text{Cl}$  (40 mL) and washed with water (30 mL  $\times$  3). The organic phase was dried over anhydrous  $\text{Na}_2\text{SO}_4$  and purified by column chromatography eluting with ethyl acetate/MeOH/ $\text{NH}_4\text{OH}$  (30:1:0.5%) to afford target compound **6a–q**.

**2-(4-(3-(Dimethylamino)propoxy)phenyl)-4H-chromen-4-one (6a)** Light yellow solid; yield: 88%, m.p.: 112–114 °C; IR (KBr,  $\text{cm}^{-1}$ )  $\nu_{\text{max}}$ : 1618 (C=O);  $^1\text{H}$  NMR ( $\text{CDCl}_3$ , 500 MHz)  $\delta$  (ppm): 8.23 (dd,  $J = 7.8$ , 1.5 Hz, 1H,  $\text{H}_5$ ), 7.88 (d,  $J = 9.0$  Hz, 2H,  $\text{H}_2'$ , and  $\text{H}_6'$ ), 7.68 (dt,  $J = 7.8$ , 1.5 Hz,

1H,  $\text{H}_7$ ), 7.56 (d,  $J = 7.8$  Hz, 1H,  $\text{H}_8$ ), 7.41 (dt,  $J = 7.8$ , 1.0 Hz, 1H,  $\text{H}_6$ ), 7.03 (d,  $J = 9$  Hz, 2H,  $\text{H}_3'$ , and  $\text{H}_5'$ ), 6.75 (s, 1H,  $\text{H}_3$ ), 4.18 (t,  $J = 6.3$  Hz, 2H,  $\text{CH}_2\text{-O}$ ), 2.55 (t,  $J = 6.7$  Hz, 2H,  $\text{CH}_2\text{-N}$ ), 2.33 (s, 6H,  $2\text{CH}_3\text{-N}$ ), 2.07–2.02 (m, 2H,  $\text{CH}_2$  aliphatic chain);  $^{13}\text{C}$  NMR ( $\text{CDCl}_3$ , 125 MHz)  $\delta$  (ppm): 178.4, 163.4, 161.8, 156.2, 133.6, 128.0, 125.7, 125.1, 123.9, 121.7, 117.9, 114.9, 106.2, 66.3, 56.2, 45.3, 27.1; anal. calcd. for  $\text{C}_{20}\text{H}_{21}\text{NO}_3$ : C, 74.28; H, 6.55; N, 4.33; found: C, 74.66; H, 6.30; N, 4.20.

**2-(4-(4-(Dimethylamino)butoxy)phenyl)-4H-chromen-4-one (6b)** Light yellow solid; yield: 80%, m.p.: 95–97 °C; IR (KBr,  $\text{cm}^{-1}$ )  $\nu_{\text{max}}$ : 1825 (C=O);  $^1\text{H}$  NMR ( $\text{CDCl}_3$ , 500 MHz)  $\delta$  (ppm): 8.23 (dd,  $J = 8.0$ , 1.5 Hz, 1H,  $\text{H}_5$ ), 7.87 (d,  $J = 8.7$  Hz, 2H,  $\text{H}_2'$ , and  $\text{H}_6'$ ), 7.68 (dt,  $J = 8.0$ , 1.5 Hz, 1H,  $\text{H}_7$ ), 7.55 (d,  $J = 8.0$  Hz, 1H,  $\text{H}_8$ ), 7.41 (dt,  $J = 8.0$ , 1.0 Hz, 1H,  $\text{H}_6$ ), 7.01 (d,  $J = 8.7$  Hz, 2H,  $\text{H}_3'$ , and  $\text{H}_5'$ ), 6.75 (s, 1H,  $\text{H}_3$ ), 4.07 (t,  $J = 6.3$  Hz, 2H,  $\text{CH}_2\text{-O}$ ), 2.41 (t,  $J = 6.7$  Hz, 2H,  $\text{CH}_2\text{-N}$ ), 2.29 (s, 6H,  $2\text{CH}_3\text{-N}$ ), 1.88–1.83 (m, 2H,  $\text{CH}_2$  aliphatic chain), 1.73–1.69 (m, 2H,  $\text{CH}_2$  aliphatic chain);  $^{13}\text{C}$  NMR ( $\text{CDCl}_3$ , 125 MHz)  $\delta$  (ppm): 179.6, 163.5, 161.9, 156.2, 133.5, 128.0, 125.6, 125.1, 123.9, 123.8, 117.9, 114.9, 106.1, 67.9, 59.2, 45.3, 26.9, 24.0; anal. calcd. for  $\text{C}_{21}\text{H}_{23}\text{NO}_3$ : C, 74.75; H, 6.87; N, 4.15; found: C, 74.26; H, 7.16; N, 4.35.

**2-(4-((5-(Dimethylamino)pentyl)oxy)phenyl)-4H-chromen-4-one (6c)** Light yellow solid; yield: 83%, m.p.: 90–92 °C; IR (KBr,  $\text{cm}^{-1}$ )  $\nu_{\text{max}}$ : 1602 (C=O);  $^1\text{H}$  NMR ( $\text{CDCl}_3$ , 500 MHz)  $\delta$  (ppm): 8.23 (dd,  $J = 7.8$ , 1.5 Hz, 1H,  $\text{H}_5$ ), 7.88 (d,  $J = 9.0$  Hz, 2H,  $\text{H}_2'$ , and  $\text{H}_6'$ ), 7.69 (dt,  $J = 7.8$ , 1.5 Hz, 1H,  $\text{H}_7$ ), 7.55 (d,  $J = 7.8$  Hz, 1H,  $\text{H}_8$ ), 7.41 (dt,  $J = 7.8$ , 1.0 Hz, 1H,  $\text{H}_6$ ), 7.01 (d,  $J = 9.0$  Hz, 2H,  $\text{H}_3'$ , and  $\text{H}_5'$ ), 6.75 (s, 1H,  $\text{H}_3$ ), 4.05 (t,  $J = 6.5$  Hz, 2H,  $\text{CH}_2\text{-O}$ ), 2.39 (bs, 2H,  $\text{CH}_2\text{-N}$ ), 2.31 (s, 6H,  $2\text{CH}_3\text{-N}$ ), 1.88–1.83 (m, 2H,  $\text{CH}_2$  aliphatic chain), 1.62–1.49 (m, 4H,  $2\text{CH}_2$  aliphatic chain);  $^{13}\text{C}$  NMR ( $\text{CDCl}_3$ , 125 MHz)  $\delta$  (ppm): 178.9, 164.2, 162.4, 156.1, 133.9, 128.3, 125.7, 124.9, 124.1, 123.5, 118.1, 115.1, 105.8, 69.8, 59.4, 44.8, 28.5, 27.1, 23.0; anal. calcd. for  $\text{C}_{22}\text{H}_{25}\text{NO}_3$ : C, 75.19; H, 7.17; N, 3.99; found: C, 75.08; H, 7.52; N, 3.75.

## AChE and BuChE inhibition assay

### In vitro inhibition studies on AChE and BuChE

AChE (E.C. 3.1.1.7, type V-S, lyophilized powder, from electric eel, 1000 U), BuChE (E.C. 3.1.1.8, from equine serum), and butyrylthiocholine iodide (BTC) were provided from Sigma-Aldrich. 5,5-Dithiobis-(2-nitrobenzoic acid) (DTNB), potassium dihydrogen phosphate, dipotassium hydrogen phosphate, potassium hydroxide, sodium hydrogen carbonate, and acetylthiocholine iodide were purchased

from Fluka. The solutions of the target compounds were prepared in a mixture of dimethyl sulfoxide (DMSO) (1 mL) and methanol (9 mL) and diluted in 0.1 M  $\text{KH}_2\text{PO}_4/\text{K}_2\text{HPO}_4$  buffer (pH 8.0) to obtain final assay concentrations. The temperature was adjusted as 25 °C during all experiments. Five different concentrations were tested for each compound in triplicate to obtain the range of 20–80% inhibition for AChE and BuChE. The assay medium was composed of 3 mL of 0.1 M phosphate buffer (pH = 8.0), 100 mL of 0.01 M DTNB, and 100 mL of 2.5 Unit/mL enzyme solution (AChE, E.C. 3.1.1.7, type V-S, lyophilized powder, from electric eel). One-hundred milliliters of each tested compound was added to the assay tube and incubated at 25 °C for 15 min prior to adding 20 mL of substrate (acetylthiocholine iodide). The rate of absorbance change was measured at 412 nm for 6 min on the baseline obtained by blank reading of the solutions with nonenzymatic hydrolysis. The blank was contained 3 mL buffer, 200 mL water, 100 mL DTNB, and 20 mL substrate. The  $\text{IC}_{50}$  values were determined graphically from inhibition curves (log inhibitor concentration versus percent of inhibition). Spectrophotometric measurements were performed on a UV Unico Double Beam Spectrophotometer (Nadri et al. 2013). The described method was also taken for the BuChE inhibition assay.

#### Determination of the inhibitory potency on the self-mediated $\text{A}\beta_{(1-42)}$ aggregation

The thioflavin-T fluorescence method was used to investigate the self-mediated  $\text{A}\beta_{(1-42)}$  aggregation (Bartolini et al. 2007; Zha et al. 2016). 1,1,1,3,3,3-Hexafluoro-2-propanol pretreated  $\text{A}\beta$  sample (Bachem company, Switzerland) was diluted in assay buffer to have a stock solution ( $[\text{A}\beta_{1-42}] = 50 \text{ mM}$ ). Experiments were performed by dissolving the peptide in phosphate buffer (pH 7.4), at 37 °C for 48 h (final  $\text{A}\beta$  concentration = 25 mM, 10 mL) with and without inhibitors. The inhibitors were solved in DMSO and diluted in the assay buffer at a final concentration of 10  $\mu\text{M}$ . Blanks containing ThT and inhibitor were prepared and evaluated to account for quenching and fluorescence properties. After incubation, 180 mL ThT (5 mM in 50 mM glycine–NaOH buffer, pH 8.5) was added to samples. The fluorescence intensities were carried out with a multimode plate reader (EnSpire, PerkinElmer, Waltham, MA, USA) at ( $\lambda_{\text{ex}} = 446 \text{ nm}$ ;  $\lambda_{\text{em}} = 490 \text{ nm}$ ), each assay was run in triplicate and each reaction was repeated at least three independent times, values at plateau were averaged after subtracting the background fluorescence of 5 mM ThT solution. The fluorescence intensities were compared and the % inhibition was calculated by the following equation:  $100 - [(\text{IF}_i - \text{IF}_b)/(\text{IF}_o - \text{IF}_b) \times 100]$  where  $\text{IF}_i$ ,  $\text{IF}_o$ , and  $\text{IF}_b$  are the fluorescence intensities obtained for

$\text{A}\beta$  aggregation in the presence of inhibitors, in the absence of inhibitors and the blanks, respectively.

#### Determination of the inhibitory potency on $\text{A}\beta_{1-40}$ aggregation induced by AChE

For co-incubation experiments of  $\text{A}\beta_{(1-40)}$  trifluoroacetate salt (Bachem company, Switzerland) and AChE from (Sigma, *Electrophorus electricus*), the mixtures of  $\text{A}\beta_{(1-40)}$  peptide and AChE in presence or absence of the test inhibitor were incubated for 24 h at room temperature (Bartolini et al. 2003; Rouleau et al. 2011). The final concentrations of  $\text{A}\beta$  (dissolved in DMSO and diluted with 0.215 M of sodium phosphate buffer, pH 8), AChE (dissolved in 0.215 M of sodium phosphate buffer, pH 8.0) and the tested compound were 200, 2, and 100  $\mu\text{M}$ , respectively. The ThT fluorescence method was used to analyze co-aggregation inhibition and the fluorescence was measured with multimode plate reader (EnSpire, PerkinElmer Waltham, MA, USA, at  $\lambda_{\text{ex}} = 446 \text{ nm}$  and  $\lambda_{\text{em}} = 490 \text{ nm}$ ). After co-incubation, 20  $\mu\text{L}$  of the solutions was diluted to a final volume of 2 mL with ThT (1.5  $\mu\text{M}$  in 50 mM glycine–NaOH buffer, pH 8.5). Blanks containing AChE,  $\text{A}\beta$ , AChE plus the tested compounds and  $\text{A}\beta$  plus the tested compounds in 0.215 M sodium phosphate buffer (pH 8.0) were prepared. The percent inhibition of the AChE-induced aggregation due to the presence of inhibitors was calculated by the following expression:  $100 - [(\text{IF}_i - \text{IF}_b)/(\text{IF}_o - \text{IF}_b) \times 100]$  where  $\text{IF}_i$ ,  $\text{IF}_o$ , and  $\text{IF}_b$  are the fluorescence intensities obtained for  $\text{A}\beta$  aggregation in the presence of inhibitors, in the absence of inhibitors and the blanks, respectively. Each assay was run in triplicate and each reaction was repeated at least three independent times.

#### Neuroprotection assay against $\text{H}_2\text{O}_2$ -induced cell death in PC12 cells

PC12 cell line was purchased from Pasteur institute. Cells were cultivated in DMEM supplemented with 10% fetal calf serum, 5% horse serum and antibiotics (100 U/mL penicillin and 100  $\mu\text{g}/\text{mL}$  streptomycin). To induce neuronal differentiation, PC12 cells were resuspended using trypsin/EDTA (0.25%) and seeded in 96-well culture plate (3000 cells/well) and cultured for 1 week in differentiation medium (DMEM + 2% horse serum + NGF (100 ng/mL) + penicillin and streptomycin). To evaluate the effect of drugs on survival rate of neurons, the culture medium was changed to NGF free medium and different concentrations of candidate drugs (10, 50, and 100  $\mu\text{M}$ ) were applied on cells. Quercetin (50  $\mu\text{M}$ ) was used as a positive control. Drugs were diluted into DMEM and added to each well in the volume of 10  $\mu\text{L}$ . Three hours after induction, ROS-mediated apoptosis was

initiated by adding the  $\text{H}_2\text{O}_2$  (400  $\mu\text{M}$ ) to the medium and after 12 h, MTT assay was performed. MTT solution (5 mg/mL) was added to each well in a volume of 10  $\mu\text{L}$ , and 3 h later culture medium was replaced with 100  $\mu\text{L}$  of DMSO. Absorbance at 545 nm was determined for each well using an ELISA reader. Each experiment was performed in four replicates. All culture media and supplements were purchased from Gibco.

## Docking studies

In order to predict the binding mode of the ligand in the active site of AChE, the docking simulation was conducted using Autodock vina (1.1.2) (Trott and Olson 2010). The 3D coordinates of AChE, (PDB ID: 1eve) was retrieved from Protein Data Bank (PDB) at <http://www.rcsb.org/pdb/home/home.do>. Preparing the protein for docking, the nonprotein atoms were omitted and minimized using OPLS3 force field (RMSD = 0.3 Å) afterwards. The size of the grid box defined for Autodock vina was 25 × 25 × 25, and the center of the box was fixed on cocystal ligand (donepezil). The best pose was selected based on the binding energy.

## Results and discussion

### Chemistry

Scheme 1 illustrated the stepwise synthesis of target compounds **6a–q**, started from cyclization reaction between 2-hydroxyacetophenone **1** and 4-methoxy benzaldehyde **2**. The reaction was carried out in the presence of pyrrolidine as a base and iodine catalyst in DMSO, affording 2-(4-

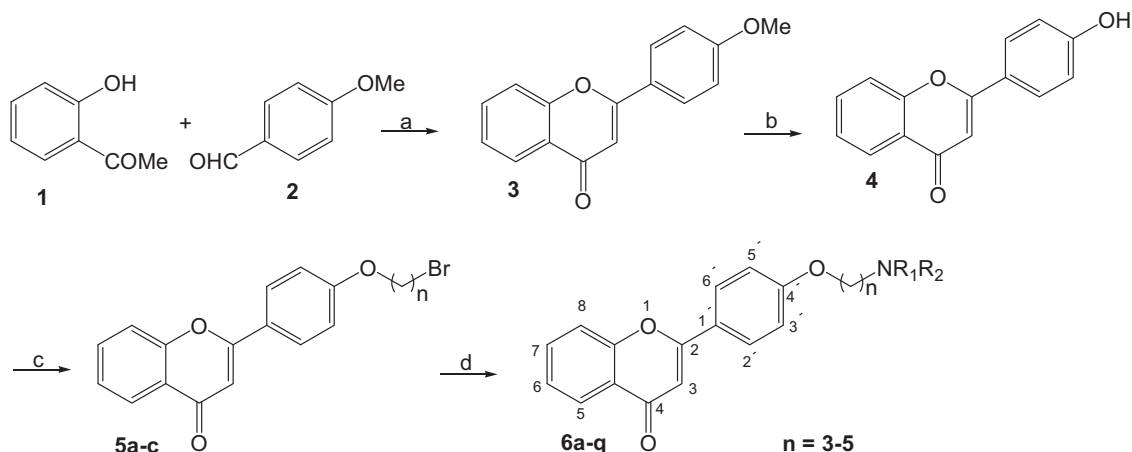
methoxyphenyl)-4H-chromen-4-one **3** in good yield (Naik et al. 2014). Treatment of compound **3** with  $\text{BBr}_3$  provided demethylated product **4** (Sagrera et al. 2011), which was converted to the corresponding alkylated products **5** via deprotonation with potassium carbonate ( $\text{K}_2\text{CO}_3$ ) in acetone and reacting with appropriate dibromoalkanes (alkyl chain length = 3, 4, and 5). The subsequent amination reaction afforded target compounds **6a–q** in good yields. Structural characterization of all target compounds was accomplished by using  $^1\text{H}$ -,  $^{13}\text{C}$ -NMR, IR spectroscopy and elemental analysis.

### Pharmacology

#### AChE and BuChE inhibitory assay

The potential of the target compounds **6a–q** for AChE (from *electric eel*) and BuChE (from *equine serum*) inhibition was screened by the Ellman's spectrophotometric method (Ellman et al. 1961).  $\text{IC}_{50}$  values for AChE and BuChE inhibition were calculated and the results are presented in Table 1. All target compounds showed suitable inhibitory activity against AChE with  $\text{IC}_{50}$  values ranging from 0.01 to 11.5  $\mu\text{M}$ . The  $\text{IC}_{50}$  values of the target compounds against BuChE demonstrated that all compounds except **6n** exhibited acceptable anti-BuChE activity.

First of all, the different carbon chain sizes containing tertiary amines, meaning dimethylamino (**6a–c**), diethylamino (**6d–f**) and pyrrolidin-1-yl (**6g–i**) were investigated. Among them, compounds **6h** ( $\text{IC}_{50}$  = 0.041  $\mu\text{M}$ ) and **6i** ( $\text{IC}_{50}$  = 0.01  $\mu\text{M}$ ) showed the best anti-AChE activities. Compound **6i** was 1.8 times stronger than reference compound, donepezil. The increasing AChE inhibitory activity was achieved by increasing the size of alkyl chain from



**Scheme 1** Synthesis of flavonoid derivatives **6a–q**. Reagents and conditions: **a** pyrrolidine,  $\text{I}_2$ , dimethyl sulfoxide, 160 °C, 24 h, 80%; **b**  $\text{BBr}_3$ , dichloromethane,  $-60\text{ }^\circ\text{C} \rightarrow \text{rt}$ , 24 h, 90%; **c**  $\text{Br}(\text{CH}_2)_n\text{Br}$ ,  $n =$

3–5, anhydrous  $\text{K}_2\text{CO}_3$ , acetone, reflux, 6 h, 88–92%; **d**  $\text{R}_1\text{R}_2\text{NH}$ ,  $\text{K}_2\text{CO}_3$ , acetonitrile, 80 °C, 10 h, 68–91%

**Table 1** Inhibitory activity of the synthesized compound **6a–q** against AChE and BuChE

Compound	n		AChE Inhibition <sup>a</sup>		SI <sup>d</sup>
			(IC <sub>50</sub> ± SD) <sup>b</sup> (μM)	BuChE Inhibition (IC <sub>50</sub> ± SD) <sup>c</sup> (μM)	
<b>6a</b>	3		0.495±0.006	6.4±0.6	12.93
<b>6b</b>	4		0.307±0.013	3.8±0.1	12.37
<b>6c</b>	5		0.260±0.022	4.4±0.3	16.92
<b>6d</b>	3		0.225±0.015	4.1±0.1	18.22
<b>6e</b>	4		0.182±0.010	2.9±0.1	15.93
<b>6f</b>	5		0.179±0.015	2.3±0.1	12.84
<b>6g</b>	3		0.115±0.004	2.7±0.1	23.47
<b>6h</b>	4		0.041±0.003	1.1±0.2	26.83
<b>6i</b>	5		0.010±0.001	2.4±0.3	240
<b>6j</b>	4		0.067±0.004	0.335±0.015	5
<b>6k</b>	4		0.140±0.008	0.854±0.005	6.1
<b>6l</b>	4		1.28±0.080	17.4±1.7	13.6
<b>6m</b>	5		0.517±0.011	16.5±0.9	31.91
<b>6n</b>	5		11.5±2.35	>100	8.69
<b>6o</b>	5		1.4±0.25	42±3.3	30
<b>6p</b>	5		0.151±0.011	3.17±0.3	20.0
<b>6q</b>	5		0.522±0.030	14.1±0.8	27.01
<b>Donepezil</b>	-		0.018±0.002	6.820±1.2	

<sup>a</sup>AChE from *Electrophorus electricus*<sup>b</sup>IC<sub>50</sub> values are at least from three independent experiments and are expressed as the means ± SD<sup>c</sup>BuChE from equine serum<sup>d</sup>SI: selectivity index = IC<sub>50</sub> (BuChE)/IC<sub>50</sub> (AChE)

three to five carbon atoms. However, this reasonable trend was not observed in case of BuChE inhibition. In this regard, four and five carbon tethers between amines and flavonoid moiety have been determined as an optimal length and subjected for examination of different amines at the end of these tethers. Among all compounds, compound **6i** bearing the pyrrolidin-1-yl moiety and compound **6j** having methylbenzyl amino group displayed the best inhibitory results against AChE and BuChE, respectively. Compounds bearing pyrrolidin-1-yl group (**6g–i**) exhibited the highest activity against AChE compared to their counterparts bearing diethylamino, dimethylamino, ethylbenzyl amino, and 4-benzylpiperidine-1-yl (**6a–f**, **6k**, **6l**). The BuChE inhibitory activity of the compounds bearing *N*-methylbenzyl and *N*-ethylbenzyl (**6j**,  $IC_{50} = 0.34 \mu\text{M}$  and **6k**,  $IC_{50} = 0.85 \mu\text{M}$ ) are respectively twenty and eight orders of magnitude more potent than donepezil ( $IC_{50} = 6.82 \mu\text{M}$ ). The change of amine groups from piperidine ring **6m** to morpholine **6n** and thiomorpholine **6o**, containing additional hetero atoms, reduced the AChE and BuChE inhibitory effects. These results indicated the importance of the hydrophobic interactions in the binding region of the enzymes which are essential for strong inhibition. Finally, the introduction of quaternary amines (**6p**, **6q**) to the end of tether did not result in better inhibitory activities compared to the pyrrolidine-containing counterparts.

### Inhibition of AChE-induced and A $\beta$ (1–42) self-induced aggregation

Regarding the role of amyloid beta A $\beta$  (1–42) aggregation in AD pathogenic cascade, the most potent AChE inhibitors were evaluated using a thioflavin T (ThT) fluorescence assay and compared with reference compound. Compounds **6h** and **6i** inhibited 42.8% and 49.2% self-induced aggregation at  $10 \mu\text{M}$  concentration, respectively, which is higher than the inhibition of donepezil (17.2%, Table 2). Moreover, the binding of AChE and A $\beta$  led to the conversion of A $\beta$  peptide into amyloid fibrils producing more toxic AChE-A $\beta$  complexes (Inestrosa et al. 1996). Structural analysis by X-ray crystallography (Bourne et al. 2003) clearly identified the PAS region of the enzyme as the locus part for interaction with A $\beta$  (Bolognesi et al. 2009). To further explore the dual action of the compounds, the inhibitory activities of compounds **6i** and **6h** towards AChE-induced A $\beta$  (1–42) peptide aggregation were investigated employing the same ThT-based fluorometric method. Compounds **6h** and **6i** demonstrated the acceptable AChE-induced A $\beta$  aggregation inhibitory effects (49.8% and 51.3% at  $100 \mu\text{M}$ , respectively) which are more efficient than donepezil (24.6%), indicating the binding of these compounds to peripheral anionic site of AChE.

**Table 2** Inhibition of self- and AChE-induced A $\beta$  aggregation by compounds **6h** and **6i**

Compound	Inhibition of A $\beta$ aggregation (%)	
	Self-induced <sup>a</sup>	AChE-induced <sup>b</sup>
<b>6h</b>	42.8 ± 2.7	49.8 ± 1.8
<b>6i</b>	49.2 ± 1.3	51.3 ± 2.6
<b>Donepezil</b>	17.2 ± 2.9	24.6 ± 1.3

<sup>a</sup>Inhibition of self-induced A $\beta$ (1–42) aggregation (25 mM) produced by the tested compound at  $10 \mu\text{M}$  concentration. Values are expressed as means ± SEM of three experiments

<sup>b</sup>Co-aggregation inhibition of A $\beta$ (1–40) and AChE ( $2 \mu\text{M}$ , ratio 100:1) by the tested compound at  $100 \mu\text{M}$  concentration was detected by ThT assay. Values are expressed as means ± SEM of three experiments

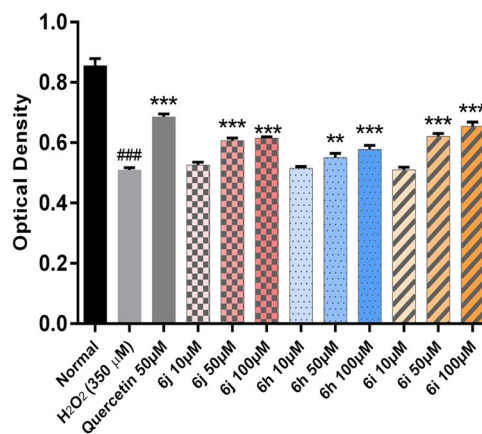


**Fig. 2** Neuroprotective activity of compound **6h–j** against  $\text{H}_2\text{O}_2$ -induced cell death in differentiated PC12 cells. Data are expressed as mean ± SD ( $n = 4$ ), \*\*\* $P < 0.001$ , \*\* $P < 0.01$  all versus  $\text{H}_2\text{O}_2$  group. ### $P < 0.001$   $\text{H}_2\text{O}_2$  versus control group

### Protection against $\text{H}_2\text{O}_2$ -induced cell death in PC12 neurons

The neuroprotective activities of three compounds (**6h**, **6i**, and **6j**) against oxidative  $\text{H}_2\text{O}_2$ -induced cell death in differentiated PC12 cells were evaluated. The data are presented in Fig. 2. Compounds **6h**, **6i**, and **6j** were evaluated at nontoxic concentration ( $<100 \mu\text{M}$ ) against PC12 cells. Based on the results, compounds **6j** (viability = 61.57%), **6h** (viability = 7.77%), and **6i** (viability = 64.45%) showed significant protective capability at  $100 \mu\text{M}$ .

### Kinetic study of AChE inhibition

The AChE inhibitory mechanism of target compounds was determined by selection of compound **6i** (the most active compound) as representative compound. The graphical analysis of Lineweaver-Burk plot was measured at different concentrations of these compound (0.575, 0.115, and  $0.23 \mu\text{M}$ ) (Fig. 3). Considering the observed pattern, the mixed type of inhibition, implying the dual binding of this

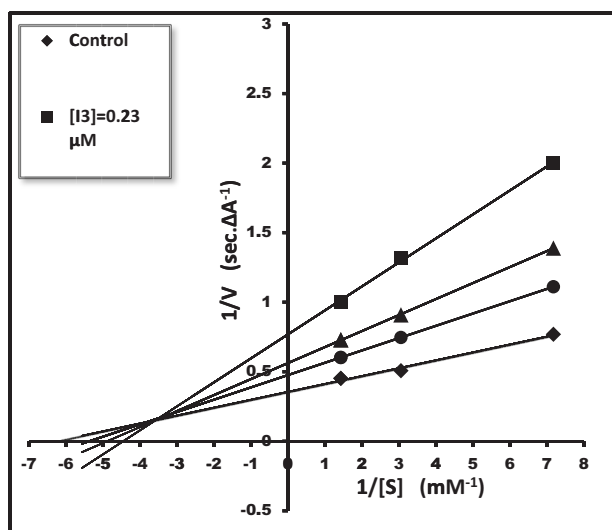


**Fig. 3** Lineweaver–Burk plot for the inhibition of AChE by compound **6i** at different concentrations of substrate

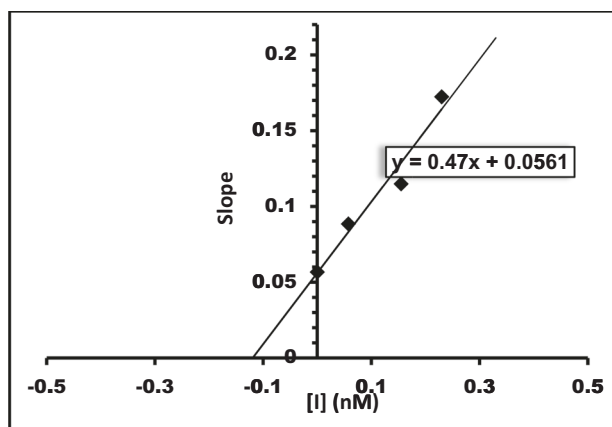


**Fig. 4** Lineweaver–Burk secondary plot for  $K_i$  calculation

compound with peripheral and catalytic anionic site, is suggested. Using the Lineweaver–Burk secondary plot (Fig. 4), 0.12  $\mu\text{M}$  was determined as  $K_i$  value for **6i**.

### Docking study

The binding pattern as depicted in Fig. 5 was retrieved from PLIP (Protein-Ligand Interaction Profiler: Python-based application) (Salentin et al. 2015). The scaffold of the target compound is composed of a tertiary or quaternary amine head linked to a flavonoid moiety through an aliphatic side chain. As shown in Fig. 6, interactions between the most potent compound **6i** and AChE include hydrogen bonds, salt bridge,  $\pi$ -stacking, and hydrophobic interactions, of which hydrogen bond and salt bridge are the most dominant ones.

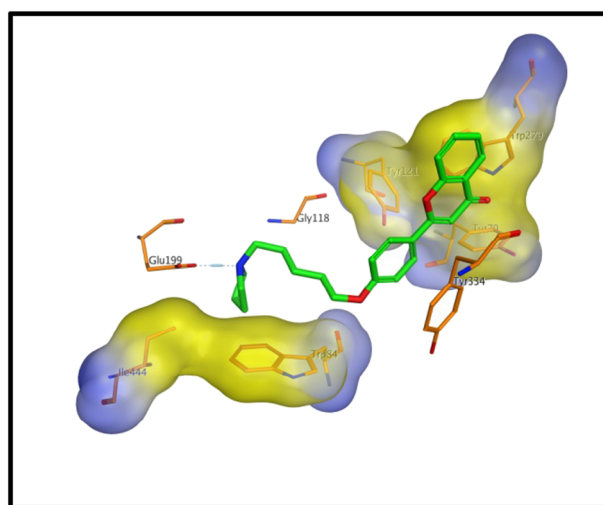


**Fig. 5** Docking pose of compound **6i** into the binding site of AChE

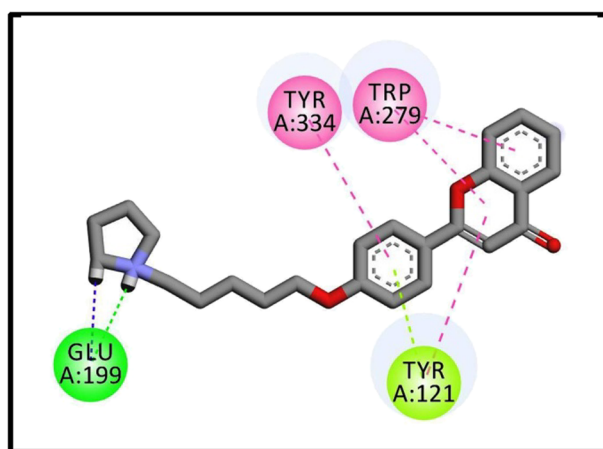


**Fig. 6** The simplified interactions between **6i** and AChE

Type of the interactions may vary between the head and the tail of the compound due to the nature of the structural components. The catalytic site of the enzyme which is occupied by the head of the compound is more involved in hydrophilic interactions. Protonated pyrrolidin moiety forms a hydrogen bond with NH group of GLY118 with average distance of 3.73 Å. In addition, GLU199 which is a component of the active site participates in a salt bridge interaction with pyrrolidine, resulting in strong binding of the ligand and displaying better inhibitory profile. The hydrophobic patch at the bottom of the gorge created by TRP84, ILE444, and TYR130 is involved in hydrophobic interactions with lipophilic part of pyrrolidine ring. Being anchored to the bottom of the gorge facilitates attachment of the molecule in the active site, in a way that flat and hydrophobic flavone moiety is directed towards PAS site of the enzyme. In this site hydrophobic and  $\pi$ -stacking interactions play a pivotal role in ligand–receptor interaction.

Flavonoid moiety is involved in  $\pi$ -stacking interaction with aromatic amino acids of PAS including TYR334 and TYR121 with average distances of 4.82 and 5.35 Å, respectively. Hydrophobic interactions between flavonoid and the two hydrophobic residues of TYR 70 and TRP279 aid the conformation to retain the stability. The figures were constructed using Discovery studio 4.5 client (Dassault Systèmes BIOVIA 2015).

## Conclusion

In conclusion, a new series of aminoalkyl-substituted flavonoids **6a–q** have been designed, synthesized and evaluated as MTDL. Compound **6i** containing pyrrolidino group linked to flavonoid scaffold via five carbon linker exhibited the most potent AChE inhibitory activity ( $IC_{50} = 0.01 \mu\text{M}$ ). Compounds **6j** and **6k** showed the highest inhibitory activity against BuChE. In addition, compounds **6h** and **6i** were tested for their ability to block the self-induced A $\beta$  and the AChE-induced A $\beta$  aggregation, exhibiting more potency than donepezil. Furthermore, the molecular modeling study of compound **6i** demonstrated the binding of aromatic part and pyrrolidin to the PAS and CAS of AChE, respectively. The in vitro neuroprotective assay of compound **6i** showed that this compound could protect neurons against H<sub>2</sub>O<sub>2</sub>-induced cell death. These findings suggest compound **6i** as the promising multifunctional agent for further study to find new anti-Alzheimer agents.

**Acknowledgements** This work was supported by Iran National Science Foundation (INSF).

## Compliance with ethical standards

**Conflict of interest** The authors declare that they have no conflict of interest.

**Publisher's note:** Springer Nature remains neutral with regard to jurisdictional claims in published maps and institutional affiliations.

## References

- Alipour M, Khoobi M, Moradi A, Nadri H, Homayouni Moghadam F, Emami S, Hasanpour Z, Foroumadi A, Shafiee A (2014) Synthesis and anti-cholinesterase activity of new 7-hydroxycoumarin derivatives. *Eur J Med Chem* 82:536–544
- Asadipour A, Alipour M, Jafari M, Khoobi M, Emami S, Nadri H, Sakhteman A, Moradi A, Sheibani V, Homayouni Moghadam F, Shafiee A, Foroumadi A (2013) Novel coumarin-3-carboxamides bearing N-benzylpiperidine moiety as potent acetylcholinesterase inhibitors. *Eur J Med Chem* 70:623–630
- Bartolini M, Bertucci C, Bolognesi ML, Cavalli A, Melchiorre C, Andrisano V (2007) Insight into the kinetic of amyloid beta (1–42) peptide self-aggregation: elucidation of inhibitors' mechanism of action. *Chembiochem* 8(17):2152–2161
- Bartolini M, Bertucci C, Cavrini V, Andrisano V (2003) beta-Amyloid aggregation induced by human acetylcholinesterase: inhibition studies. *Biochem Pharmacol* 65(3):407–416
- Bartus RT, Dean RL, Beer B, Lippa AS (1982) The cholinergic hypothesis of geriatric memory dysfunction. *Science* 217:408–417
- Bolognesi ML, Cavalli A, Melchiorre C (2009) Memoquin: a multi-target-directed ligand as an innovative therapeutic opportunity for Alzheimer's disease. *Neurotherapeutics* 6(1):152–162
- Bourne Y, Taylor P, Radic Z, Marchot P (2003) Structural insights into ligand interactions at the acetylcholinesterase peripheral anionic site. *EMBO J* 22(1):1–12
- Dassault Systèmes BIOVIA (2015) Discovery studio modeling environment, Release 4.5. Dassault Systèmes, San Diego
- Ellman GL, Courtney KD, Andres V, Featherstone RM (1961) A new and rapid colorimetric determination of acetylcholinesterase activity. *Biochem Pharmacol* 7(2):88–95
- Fernàndez-Busquets X (2013) Amyloid fibrils in neurodegenerative diseases: villains or heroes? *Future Med Chem* 5(16):1903–1906
- Ghanei-Nasab S, Khoobi M, Hadizadeh F, Marjani A, Moradi A, Nadri H, Emami S, Foroumadi A, Shafiee A (2016) Synthesis and anticholinesterase activity of coumarin-3-carboxamides bearing tryptamine moiety. *Eur J Med Chem* 121:40–46
- Giacobini E (2004) Cholinesterase inhibitors: new roles and therapeutic alternatives. *Pharmacol Res* 50(4):433–440
- Greig NH, Utsuki T, Yu Q, Zhu X, Holloway HW, Perry T, Lee B, Ingram DK, Lahiri DK (2001) A new therapeutic target in Alzheimer's disease treatment: attention to butyrylcholinesterase. *Curr Med Res Opin* 17(3):159–165
- Hardy J, Selkoe DJ (2002) The amyloid hypothesis of Alzheimer's disease: progress and problems on the road to therapeutics. *Science* 297(5580):353–356
- He X, Park HM, Hyung SJ, DeToma AS, Kim C, Ruotolo BT, Lim MH (2012) Exploring the reactivity of flavonoid compounds with metal-associated amyloid- $\beta$  species. *Dalton Trans* 41:6558–6566
- Huang L, Shi A, He F, Li X (2010) Synthesis, biological evaluation, and molecular modeling of berberine derivatives as potent acetylcholinesterase inhibitors. *Bioorg Med Chem* 18(3):1244–1251
- Inestrosa NC, Alvarez A, Perez CA, Moreno RD, Vicente M, Linker C, Casanueva OI, Soto C, Garrido J (1996) Acetylcholinesterase accelerates assembly of amyloid- $\beta$ -peptides into Alzheimer's fibrils: possible role of the peripheral site of the enzyme. *Neuron* 16(4):881–891
- Jalili-Baleh L, Babaei E, Abdpour Sh, Bukhari SNA, Foroumadi A, Ramazani A, Sharifzadeh M, Abdollahi M, Khoobi M (2018) A review on flavonoid-based scaffolds as multi-target-directed ligands (MTDLs) for Alzheimer's disease. *Eur J Med Chem* 152:570–589
- Katalinic M, Rusak G, Domacinovic Barovic J, Sinko G, Jelic D, Antolovic R, Kovarik Z (2010) Structural aspects of flavonoids as inhibitors of human butyrylcholinesterase. *Eur J Med Chem* 45(1):186–192
- Li RS, Wang XB, Hu XJ, Kong LY (2013a) Design, synthesis and evaluation of flavonoid derivatives as potential multifunctional acetylcholinesterase inhibitors against Alzheimer's disease. *Bioorg Med Chem Lett* 23(9):2636–2641
- Li SY, Wang XB, Xie SS, Jiang N, Wang KDG, Yao HQ, Sun HB, Kong LY (2013b) Multifunctional tacrine-flavonoid hybrids with cholinergic,  $\beta$ -amyloid-reducing, and metal chelating properties for the treatment of Alzheimer's disease. *Eur J Med Chem* 69:632–646
- Longo FM, Massa SM (2004) Neuroprotective strategies in Alzheimer's disease. *NeuroRx* 1(1):117–127
- Lou H, Fan P, Perez RG, Lou H (2011) Neuroprotective effects of linarin through activation of the PI3K/Akt pathway in amyloid- $\beta$ -induced neuronal cell death. *Bioorg Med Chem* 19(13):4021–4027

- Lu W, Chen Y, Wang T, Hong Ch, Chang LP, Chang CC, Yang YCh, Xie SQ, Wang C (2016) Design, synthesis and evaluation of novel 7-aminoalkyl-substituted flavonoid derivatives with improved cholinesterase inhibitory activities. *Bioorg Med Chem* 24(4):672–680
- Luo W, Li YP, He Y, Huang SL, Tan JH, Ou TM, Li D, Gu LQ, Huang ZS (2011) Design, synthesis and evaluation of novel tacrine-multialkoxybenzene hybrids as dual inhibitors for cholinesterases and amyloid beta aggregation. *Bioorg Med Chem* 19(2):763–770
- Luo W, Su YB, Hong Ch, Tian RG, Su LP, Wang YQ, Li Y, Yue JJ, Wang CJ (2013) Design, synthesis and evaluation of novel 4-dimethylamine flavonoid derivatives as potential multi-functional anti-Alzheimer agents. *Bioorg Med Chem* 21(23):7275–7282
- Masters CL, Simms G, Weinman NA, Multhaup G, McDonald BL, Beyreuther K (1985) Amyloid plaque core protein in Alzheimer disease and Down syndrome. *Proc Natl Acad Sci USA* 82(12):4245–4249
- Mehrabi F, Pourshojaei Y, Moradi A, Sharifzadeh M, Khosravani L, Sabourian R, Rahmani-Nezhad S, Mohammadi-Khanaposhtani M, Mahdavi M, Asadipour A, Rahimi HR, Moghimi S, Foroumadi A (2017) Design, synthesis, molecular modeling and anticholinesterase activity of benzylidene-benzofuran-3-ones containing cyclic amine side chain. *Future Med Chem* 9(7):659–671
- Nadri H, Pirali-Hamedani M, Moradi A, Sakhteman A, Vahidi A, Sheibani V, Asadipour A, Hosseinzadeh N, Abdollahi M, Shafiee A, Foroumadi A (2013) 5,6-Dimethoxybenzofuran-3-one derivatives: a novel series of dual acetylcholinesterase/butrylcholinesterase inhibitors bearing benzyl pyridinium moiety. *DARU J Pharm Sci* 21(1):15–23
- Naik MM, Tilve SG, Kamat VP (2014) Pyrrolidine and iodine catalyzed domino aldol-Michael-dehydrogenative synthesis of flavones. *Tetrahedron Lett* 55(22):3340–3343
- Panek D, Wichur T, Godyn J, Pasiaka A, Malawska B (2017) Advances toward multifunctional cholinesterase and  $\beta$ -amyloid aggregation inhibitors. *Future Med Chem* 9(15):1835–1854
- Piazzini L, Rampa A, Bisi A, Gobbi S, Belluti F, Cavalli A, Bartolini M, Andrisano V, Valenti P, Recanatini M (2003) 3-(4-([Benzyl(methyl)amino]methyl)phenyl)-6,7-dimethoxy-2H-2-chromenone (AP2238) inhibits both acetylcholinesterase and acetylcholinesterase-induced  $\beta$ -amyloid aggregation: a dual function lead for Alzheimer's disease therapy. *J Med Chem* 46(12):2279–2282
- Pourabdi L, Khoobi M, Nadri H, Moradi A, Homayouni Moghadam F, Emami S, Mojtahedi MM, Haririan I, Forootanfar H, Ameri A, Foroumadi A, Shafiee A (2016) Synthesis and structure-activity relationship study of tacrine-based pyrano[2,3-c]pyrazoles targeting AChE/BuChE and 15-LOX. *Eur J Med Chem* 123:298–308
- Praticò D (2008) Oxidative stress hypothesis in Alzheimer's disease: a reappraisal. *Trends Pharmacol Sci* 29(12):609–615
- Rouleau J, Iorga BI, Guillou C (2011) New potent human acetylcholinesterase inhibitors in the tetracyclic triterpene series with inhibitory potency on amyloid  $\beta$  aggregation. *Eur J Med Chem* 46(6):2193–2205
- Sagrera G, Bertucci A, Vazquez A, Seoane G (2011) Synthesis and antifungal activities of natural and synthetic bioflavonoids. *Bioorg Med Chem* 19(10):3060–3073
- Salentin S, Schreiber S, Haupt VJ, Adasme MF, Schroeder M (2015) PLIP: fully automated protein-ligand interaction profiler. *Nucleic Acids Res* 43(W1):W443–W447
- Scarpini E, Scheltens P, Feldman H (2003) Treatment of Alzheimer's disease: current status and new perspectives. *Lancet Neurol* 2(9):539–547
- Selkoe DJ (1999) Translating cell biology into therapeutic advances in Alzheimer's disease. *Nature* 399(6738 Suppl):A23–31
- Sheng R, Lin X, Zhang J, Chol KS, Huang W, Yang B, He Q, Hu Y (2009) Design, synthesis and evaluation of flavonoid derivatives as potent AChE inhibitors. *Bioorg Med Chem* 17:6692–6698
- Singh M, Kaur M, Silakari O (2014) Flavones: an important scaffold for medicinal chemistry. *Eur J Med Chem* 84:206–239
- Trippier PC, Jansen Labby K, Hawker DD, Mataka JJ, Silverman RB (2013) Target- and mechanism-based therapeutics for neurodegenerative diseases: strength in numbers. *J Med Chem* 56(8):3121–3147
- Trott O, Olson AJ (2010) AutoDock Vina: improving the speed and accuracy of docking with a new scoring function, efficient optimization and multithreading. *J Comput Chem* 31(2):455–461
- Tumiatti V, Minarini A, Bolognesi ML, Milelli A, Rosini M, Melchiorre C (2010) Tacrine derivatives and Alzheimer's disease. *Curr Med Chem* 17(17):1825–1838
- Uriarte-Pueyo I, Calvo MI (2011) Flavonoids as acetylcholinesterase inhibitors. *Curr Med Chem* 18(34):5289–5302
- Viau CJ, Curren RD, Wallace K (1993) Cytotoxicity of tacrine and velnacrine metabolites in cultured rat, dog and hepatocytes. *Drug Chem Toxicol* 16(3):227–239
- Williams RJ, Spencer JPE (2012) Flavonoids, cognition, and dementia: actions, mechanisms, and potential therapeutic utility for Alzheimer disease. *Free Radical Biol Med* 52(1):35–45
- Xie Q, Wang H, Xia Z, Lu M, Zhang W, Wang X, Fu W, Tang Y, Sheng W, Li W, Zhou W, Zhu X, Qiu Z, Chen H (2008) Bis(-)-nor-meptazinols as novel nanomolar cholinesterase inhibitors with high inhibitory potency on amyloid- $\beta$  aggregation. *J Med Chem* 51(7):2027–2036
- Yankner BA, Dawes LR, Fisher S, Villa-Komaroff L, Oster-Granite ML, Neve RL (1989) Neurotoxicity of a fragment of the amyloid precursor associated with Alzheimer's disease. *Science* 245(4916):417–420
- Zha G-F, Zhang C-P, Qin H-L, Jantan I, Sher M, Amjad MW, Hussain MA, Hussain Z, Bukhari SNA (2016) Biological evaluation of synthetic  $\alpha,\beta$ -unsaturated carbonyl based cyclohexanone derivatives as neuroprotective novel inhibitors of acetylcholinesterase, butyrylcholinesterase and amyloid- $\beta$  aggregation. *Bioorg Med Chem* 24(10):2352–2359